

A new characterization of chaos from a time series



P.R.L. Alves*, L.G.S. Duarte, L.A.C.P. da Mota

Universidade do Estado do Rio de Janeiro, Instituto de Física, Depto. de Física Teórica, 20559-900 Rio de Janeiro RJ, Brazil

ARTICLE INFO

Article history:

Received 12 July 2017

Revised 28 July 2017

Accepted 29 August 2017

Keywords:

Chaos

Time series

Algebraic computation

ABSTRACT

In the reconstruction scheme, the global fitting is a basis for the approach to the time evolution of dynamic systems directly from time series. A new theory of dynamic characterization is present in the aim of this work. The least squares method determines the predictors in the Algebraic Computation environment. The program for diagnosing of time series run in a Maple environment. The computational routine determines a new quantifier of chaos. A test for theory and computational tools in periodic, chaotic and random systems is in the scope of this paper. An application of the method in a real-world time series gives a satisfactory result.

© 2017 Elsevier Ltd. All rights reserved.

1. Introduction

To treat the diagnosis of a series for the presence of chaos or randomness – i.e. without deterministic dynamics –, the scheme of phase space reconstruction has the solid mathematical basis from the theorems proved by Takens [1]. They provide the sufficient conditions for the embedding of a set of observables into a Euclidean space [2].

An attractor is chaotic if it has a positive Lyapunov exponent [2–4]. In fact, there are algorithms for the calculation of these exponents in the literature [5,6]. However, in a reconstructed phase space, this kind of propose requires sophisticated procedures for implementation [7–9].

This paper presents a direct method for detecting and quantifying chaos from time series. The next section treats the theoretical development of this work. Its basis is the *global approach* in the symbolic computation environment [10,11]. In this context, this theory leads to both graphical and analytical characterization of the dynamics. Our computational program permits to investigate simulated series and observables of the real world in the third part of this work.

2. Theoretical development

At this initial stage, we attempt to construct a mapping between different states. This map is a function of coordinates in the phase space reconstructed. Being $|\alpha(t)\rangle$ a state vector corresponding to time t , the function f_τ relates $|\alpha(t)\rangle$ with the state $|\alpha(t + \tau \Delta t)\rangle$ [12]. The future time is computed by the product of an integer τ

by a time interval Δt plus the instant t , i.e. $\tau \Delta t + t$. The proposal is to find some functions $\mathcal{P}_\tau(|\alpha\rangle)$ that should be satisfactory approximations to f_τ .

$$|\alpha(t + \tau \Delta t)\rangle = f_\tau(|\alpha(t)\rangle) \quad (1)$$

This approach of the time series is a kind of *inverse problem*. Casdagli [13] expects a scaling law based on the largest Lyapunov exponent λ_{\max} :

$$\sigma_\tau = \sigma_1 e^{\tau \Delta t \lambda_{\max}}. \quad (2)$$

If the deviations σ_τ among the actual value and the numerical result of the application $\mathcal{P}_\tau(|\alpha\rangle)$ grow exponentially for $\tau \rightarrow +\infty$, then the system is chaotic. On the other hand, in the absence of chaos, there is no reason for increasing of these deviations over time, like in the completely random time series and also in periodic systems. But the accuracy of forecasts in dynamic systems with periodicity is greater than the predictability in random time series, e.g. a set of balls drawn in a lottery.

2.1. The global approach

We have described in detail the procedure for determining the global map from the reconstructed state vectors if one intends to forecast an observable [11,14]. At first, the time series $\{X(0), X(\Delta t), \dots, X((N-1)\Delta t)\}$ formed by N scalar quantities – separated by time intervals Δt – is the sole source of information about a dynamic system. In a d_E -dimensional reconstructed phase space, the components of the r -th state vector $|\alpha_r(t)\rangle$ are

* Corresponding author.

E-mail address: pauloricardo07121969@gmail.com (P.R.L. Alves).

data stored in this ordered set [15].

$$|\alpha_r(t)\rangle \doteq \begin{bmatrix} X(r(d_E T)\Delta t) \\ \vdots \\ X(r(2T)\Delta t) \\ X(rT\Delta t) \end{bmatrix} \quad (3)$$

For the reconstruction of state space, the *delays method* widely is used. In this scheme, the difference in the number of observables T between adjacent components of the state vectors (3) is the *time lag* [8]. This reconstruction's technique permits an investigation of the time evolution of one observable from geometrical quantities [15].

The embedding parameter is the product of T by the *embedding dimension* d_E ¹. The trial and error – by computational routines – in prediction is proper to decide if the product $d_E T$ is according to a good embedding in phase space or not [8].

The application of the predictor $\mathcal{P}_\tau(|\alpha_r\rangle)$ – in a *global technique*, it has a standard form [13] – results in the expected value $X_{1P(r+\tau)}$. The calculus of the deviations and errors uses the first component of state vector $|\alpha_r\rangle$. The *error in the forecast* $\epsilon_{r+\tau}$ is computed by the *true value* $X((r+\tau)(d_E T)\Delta t) \equiv X_{true}$ minus the expected value: $\epsilon_{r+\tau} = X_{true} - X_{1P(r+\tau)}$. An example of a polynomial predictor of degree five – in a three-dimensional reconstructed space – is

$$\mathcal{P}_\tau(X_{1r}, X_{2r}, X_{3r}) = c_1 X_{1r} + c_2 X_{2r} + c_3 X_{3r} + \dots + c_{55} X_{3r}^5. \quad (4)$$

The fifty-five coefficients in the polynomial above have control in the predictability.

To determine the predictor's coefficients – i.e. the components of the vector $|c\rangle$ –, one can apply the *least squares method* for minimization of a cost function $\mathcal{F}(|c\rangle)$. A set $\{|X_f\rangle\}$ of M reconstructed vectors takes part in the minimization. The cost functions are linear combinations of functions $\phi_i(|X_f\rangle)$ [11,14].

$$\mathcal{F}(|c\rangle) = \sum_{f=1}^M (\epsilon_f)^2 = \sum_{f=1}^M \left(X_{1f} - \sum_{i=1}^l c_i \phi_i(|X_{f-\tau}\rangle) \right)^2 \quad (5)$$

Above, the *residual* in a global mapping is given by

$$\epsilon_f = X(\hat{r}(d_E T)\Delta t) - X((\hat{r}-\tau)(d_E T)\Delta t) \equiv X_{1f} - X_{1(\hat{r}-\tau)}.$$

For the purpose of the dynamic characterization, the deviation σ_τ is the fundamental quantity. It is a calculation based on the sample variance [11,14].

$$\sigma_\tau = \sqrt{\frac{\sum_{f=1}^M (X_{1f} - \sum_{i=1}^l c_i \phi_i(|X_{f-\tau}\rangle))^2}{M-1}} \quad (6)$$

2.2. Dynamical characterization

The method developed consists in the analysis of the time evolution of the deviation σ_τ . In the characterization of the dynamics, we built the quantity *accuracy for a prediction time* \mathcal{A}_τ . It's the ratio of an average of absolute values and the permissible error – i.e. $3\sigma_\tau$ – in a forecast. The other quantifier used is the *relative deviation for a prediction time*, denoted by \mathcal{D}_τ . It compares the deviations calculated from the predictors $\mathcal{P}_\tau(|X_r\rangle)$ and $\mathcal{P}_1(|X_r\rangle)$.

$$\mathcal{A}_\tau = \frac{\sum_{f=1}^{M-1} |X_{1f}|}{3(M-1)\sigma_\tau} \quad (7)$$

$$\mathcal{D}_\tau = \frac{\sigma_\tau}{\sigma_1} \quad (8)$$

¹ From Takens' Theorems, a compact manifold of dimension m can be embedded into a Euclidean space which has dimension $d_E = 2m + 1$ [1,2].

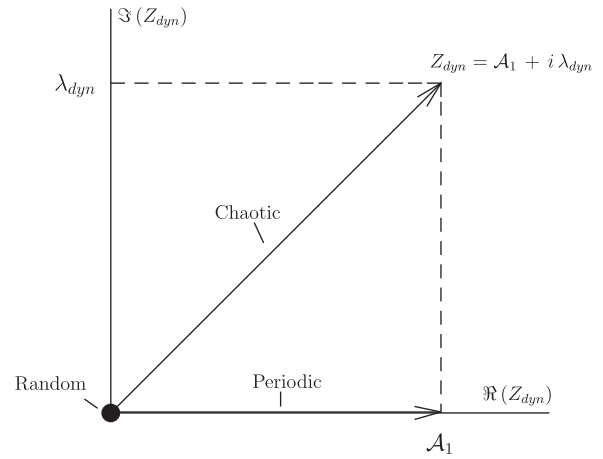


Fig. 1. Argand diagram for the new quantifier of chaos Z_{dyn} . The typical dynamics are according to results with realistic global fittings.

In a diagram, we put the “bullet” as the symbol (\bullet) for the result of $\ln(\mathcal{A}_\tau)$ and “circle” (\circ) to the value of $\ln(\mathcal{D}_\tau)$ against the parameter τ . We called it *Diagram Accuracy-Deviation*. We expect to achieve three typical cases²:

- For chaotic systems, the accuracy decays and the deviations grow in accord to the increasing of the prediction's time $\tau \Delta t$;
- When the time series is periodic, a “bullet band” is formed in the upper part of the diagram while the circles fill the under-side;
- If the series presents no determinism, the deviations remain as in the periodic case whereas the accuracy is small for any time of prediction.

Algorithms for determining the Lyapunov exponent from data requires much care or tests for evaluation of divergence between nearby trajectories in reconstructed phase spaces [7,8]. Here, we consider that a construction of a new quantifier of chaos can provide an efficient alternative to characterize the dynamics from a time series.

In a chaotic system, for instance, one expects an exponential decay like $\ln(\mathcal{A}_\tau) = \{\ln(\mathcal{A}_1)\}e^{-\hat{\lambda}\tau}$ ($\hat{\lambda} > 0$). However, this functional form may not be appropriate to fit the curve $\ln(\mathcal{A}_\tau)$. A mean of solving this problem is to disconnect these two quantities in this stage of our construction. So instead of determining a constant like $\hat{\lambda}$, we make the swap $\hat{\lambda} \rightarrow \lambda_{dyn}$. Defining λ_{dyn} as a mean,

$$\lambda_{dyn} = \sum_{\tau=1}^{N-1} \frac{\mathcal{A}_\tau - \mathcal{A}_{\tau+1}}{N-1} \quad (9)$$

the attributes of the time evolution are easily recognisable. Another advantage is that this quantity still takes into account the inevitable statistical fluctuations in the global fitting.

In fact, the nature of the dynamics leaves a record in the set of N statistical quantities $\{\mathcal{A}_1, \mathcal{A}_2, \dots, \mathcal{A}_N\}$. The independent magnitudes $\{\mathcal{A}_1, \lambda_{dyn}\}$ summarize this kind of information about the dynamic system. They admit a representation in the orthogonal axis from a Cartesian plane. Using the convenience of the complex numbers, our quantifier of chaos is

$$Z_{dyn} = \mathcal{A}_1 + i \lambda_{dyn}, \quad (10)$$

where i is the imaginary unit.

² In addition to chaotic time series, we included periodic and random series because their statistical quantifiers must present asymptotic behaviors for $\{\ln(\mathcal{A}_1) \rightarrow +\infty, \lambda_{dyn} \rightarrow 0\}$ and $\{\ln(\mathcal{A}_1) \rightarrow 0, \lambda_{dyn} \rightarrow 0\}$, respectively. Here, there is no attempt of to establish a classification of dynamics from Diagrams Accuracy-Deviation. The typical cases play a role as a guide for the interpretation of the dynamical characteristic from graphics.

Table 1
Typical dynamics for ideal global mappings.

Characterization	$\ln(A_\tau)$	$\ln(D_\tau)$	Statistical quantity	
			$\ln(A_1)$	λ_{dyn}
Chaotic	Decreasing curve	Increasing curve	$+\infty$	> 0
Random	Lower band	Lower band	0	0
Periodic	Upper band	Lower band	$+\infty$	0

The typical dynamics have an enlightening representation in the Argand diagram. In Fig. 1, the magnitude corresponds to realistic global mappings. So A_1 has finite values and λ_{dyn} is close to zero for periodic and random time series. Table 1 summarizes the expected results for ideal global fittings.

3. Results and discussions

The computational procedure DynCharTS provides all graphics and numerical results in this section. It incorporates the core of the LinMapTS package [14]. Each parameter requires a global mapping. In the Maple input below, the argument PT=16 specifies the parameter τ . So the routine determines sixteen pre-

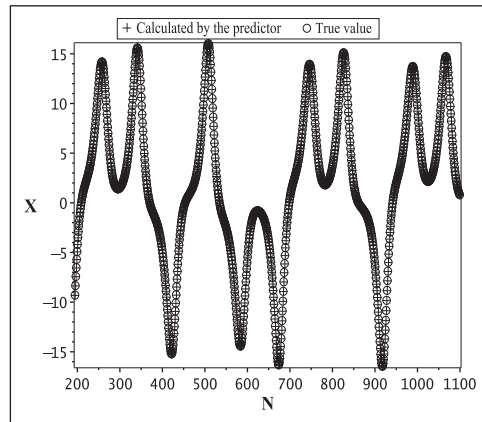
dictors in this case. The outputs are a graphical analysis of the fit and the quantifier of chaos Z_{dyn} .

```
[> Z[dyn]:=DynCharTS(DataFile='LorenzX.txt',
Degree=5,PT=16);
```

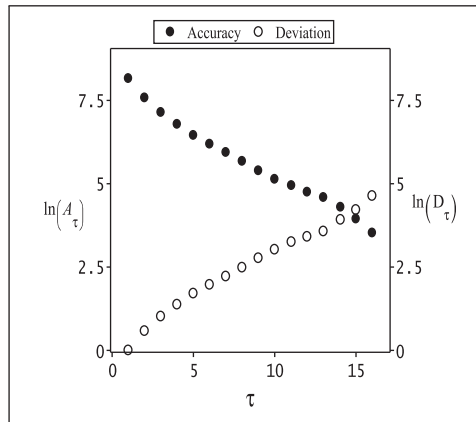
This command refers to a time series for a Lorenz System. It was generated by the routine `lorenz` of the Tisean package [16]. The file 'LorenzX.txt' stores 1,200 data that covers 12 units of time. This routine provides the Lyapunov exponents: 0.9659, -0.0467 and -13.9133 in 1/unit time. Thus, one concludes that this system is chaotic because it has a positive Lyapunov exponent [2–4].

Fig. 2(a) shows a graphical analysis for the predictor (4) – the argument Degree=5 specifies this polynomial form. There is an excellent accord between predicted and real value for the dynamical variable X. The corresponding Diagram Accuracy-Deviation (see Fig. 2(b)) and the result $Z_{dyn} = 3500 + i307$ confirm the chaotic nature of this series.

The next three case studies adopt the same model (4) and follow the previous procedure. In order to test the power of our diagram, we use a typical electrical signal as the generator of the periodic series and the results of a lottery as a random time series. They both also have 1200 data.

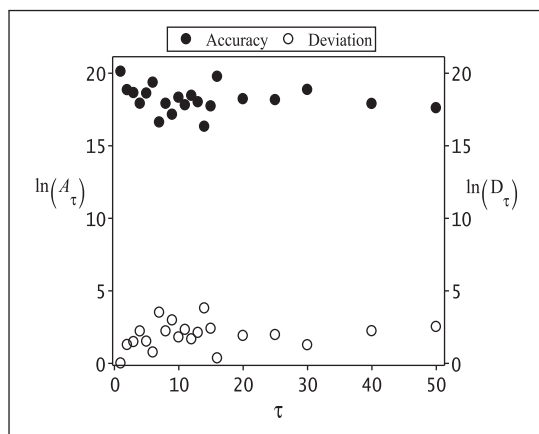


(a) Dynamical variable X versus data-order N .

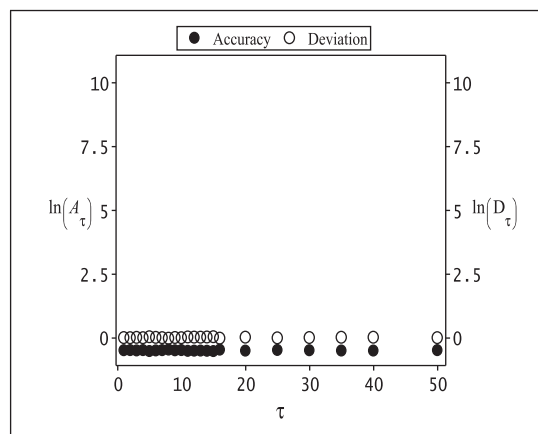


(b) Diagram Accuracy-Deviation.

Fig. 2. Graphics for the predictor (4) applied in the time series for a Lorenz System. (a) Predicted values have good agreement with the actual data. (b) The increasing of the deviation and the declining of the accuracy shows that this time series is chaotic.



(a) Periodic signal $g(t) = 3 \sin(4\pi t) + 7 \cos(3\pi t)$.



(b) Completely random time series from a lottery.

Fig. 3. Dynamical characterization by the Diagrams Accuracy-Deviation. (a) The bands of high-accuracy and deviation practically constant agree with the forecasts expected for a periodic signal. (b) The low-accuracy band in this study case is fully compatible with a random system that has not a deterministic dynamics.

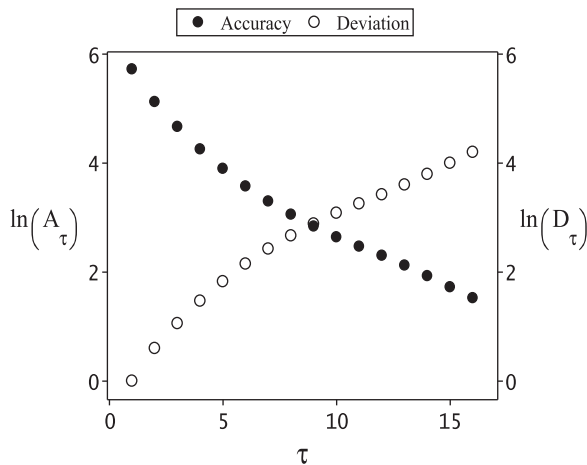


Fig. 4. Diagram Accuracy-Deviation for the chaotic signal. The accuracy and deviation curves – decreasing and increasing respectively – mark the presence of chaos.

The periodic function $g(t)$ that covers 24 units of time is $g(t) = 3 \sin(4\pi t) + 7 \cos(3\pi t)$ [17]. The first balls drawn in a Brazilian lottery were ordered to form the random series. This lottery usually pays the highest premiums if the player hits six numbers among the sixty possible scores [18].

These two series – periodic and random – constitute tests for the program. If the routine does not detect chaos, the quantity Z_{dyn} is nonsense. But the program still prints the Diagrams Accuracy-Deviation. The result also is according to the theoretical prediction, i.e. the diagrams of the Fig. 3 confirm the behavior expected in Table 1.

In the diagram for the Lorenz System, it has obtained a signature of chaos (see Fig. 2(b)) by the simultaneous decay of the accuracy and well-defined growth of the deviation. The characterization method developed in this work also is applicable to time series from real systems. Our proposal here is to analyze the results of predictions and diagrams in the case of a chaotic voltage [19,20]. Again, the curves of accuracy and deviations in Fig. 4 are in according to Table 1. In this experimental system – a chaotic circuit –, the result for the quantifier of chaos was $Z_{dyn} = 319.8 + i28.3$. Then, this result is favorable to our theory too.

4. Conclusion

The global approach in time series analysis is a technique constructed on a firm mathematical basis besides having the convenience of the symbolic computation. In the method developed in this work, the Diagrams Accuracy-Deviation and the quantifier Z_{dyn} were able to detect the dynamic characteristic, both the series generated by simulation and the time series of real-world systems.

So the theory and the computational routines presented in this paper are proper to detect chaos from a time series directly. It encourages the incorporation of this alternative to Lyapunov exponents in the investigation of complex phenomena.

Acknowledgement

L.G.S. Duarte and L.A.C.P. da Mota wish to thank Fundação de Amparo à Pesquisa do Estado do Rio de Janeiro (FAPERJ) (Registro no. 8.182/UERJ/2013 and DELIBERAÇÃO No. 25/2013) for the Research Grant.

References

- [1] Takens F. Dynamical systems and turbulence. In: Warwick 1980, vol. 898 of lecture notes in mathematics. Heidelberg: Springer Berlin; 1981. p. 366–81. <http://link.springer.com/chapter/10.1007>.
- [2] Ott E. Coping with chaos : analysis of chaotic data and the exploitation of chaotic systems. New York: J. Wiley; 1994. <https://www.amazon.es/Coping-Chaos-Analysis-Exploitation-Nonlinear/dp/0471025569>.
- [3] Grebogi C, Ott E, Pelikan S, Yorke JA. Strange attractors that are not chaotic. *Physica D* 1984;13(12):261–8. <http://www.sciencedirect.com/science/article/pii/0167278984902823>.
- [4] Kennedy JA, Stockman DR. Chaotic equilibria in models with backward dynamics. *J Econ Dyn Control* 2008;32(3):939–55. <http://www.sciencedirect.com/science/article/pii/S0165188907001066>.
- [5] Wolf A, Swift JB, Swinney HL, Vastano JA. Determining Lyapunov exponents from a time series. *Physica D* 1985;16(3):285–317. <http://www.sciencedirect.com/science/article/pii/0167278993900099>.
- [6] Rosenstein MT, Collins JJ, Luca CJD. A practical method for calculating largest Lyapunov exponents from small data sets. *Physica D* 1993;65(12):117–34. <http://www.sciencedirect.com/science/article/pii/0167278993900099>.
- [7] Sprott J. Chaos and time-series analysis. Oxford New York: Oxford University Press; 2003. <https://global.oup.com/academic/product/chaos-and-time-series-analysis-9780198508397?cc=br&lang=en&>.
- [8] Kantz H, Schreiber T. Nonlinear time series analysis. Cambridge nonlinear science series, Cambridge University Press; 2004. <http://www.cambridge.org/br/academic/subjects/physics/nonlinear-science-and-fluid-dynamics/nonlinear-time-series-analysis-2nd-edition?format=PB>.
- [9] Parlitz U. Identification of true and spurious Lyapunov exponents from time series. *Int J Bifurc Chaos* 1992;02(01):155–65. <http://www.worldscientific.com/doi/pdf/10.1142/S0218127492000148>.
- [10] Carli H, Duarte L, Mota Ld. A maple package for improved global mapping forecast. *Comput Phys Commun* 2014;185(3):1115–29. <http://www.sciencedirect.com/science/article/pii/S0010465513000413X>.
- [11] Alves P, Duarte L, Mota Ld. Improvement in global forecast for chaotic time series. *Comput Phys Commun* 2016;207:325–40. <http://www.sciencedirect.com/science/article/pii/S0010465516301278>.
- [12] Farmer JD, Sidorowich JJ. Predicting chaotic time series. *Phys Rev Lett* 1987;59:845–8. <http://journals.aps.org/prl/abstract/10.1103/PhysRevLett.59.845>.
- [13] Casdagli M. Nonlinear prediction of chaotic time series. *Physica D* 1989;35(3):335–56. <http://www.sciencedirect.com/science/article/pii/0167278989900742>.
- [14] Alves P, Duarte L, Mota Ld. Alternative predictors in chaotic time series. *Comput Phys Commun* 2017;215:265–8. <http://www.sciencedirect.com/science/article/pii/S0010465517300656?np=y&npKey=2398b0d2158d6e0d3cb54640ce7e7c61b5350119da4195aa531c7a57ba835b96>.
- [15] Ruelle D. Chaotic evolution and strange attractors : the statistical analysis of time series for deterministic nonlinear systems. Cambridge New York: Cambridge University Press; 1989. <http://www.cambridge.org/catalogue/catalogue.asp?isbn=9780521368308>.
- [16] Hegger R, Kantz H, Schreiber T. Practical implementation of nonlinear time series methods: the TISEAN package. *Chaos* 1999;9(2):413–35. <http://scitation.aip.org/content/aip/journal/chaos/9/2>.
- [17] Mandal M. Continuous and discrete time signals and systems. Cambridge, UK New York: Cambridge University Press; 2007. <http://www.cambridge.org/catalogue/catalogue.asp?isbn=9780521854559>.
- [18] Mega-Sena - Download de todos os resultados, Caixa Econômica Federal, Brazil. <http://www1.caixa.gov.br/loterias/loterias/megasena/download.aspl> (accessed 13.09.14).
- [19] Brown R, Rulkov NF, Tracy ER. Modeling and synchronizing chaotic systems from time-series data. *Phys Rev E* 1994;49:3784–800. <http://journals.aps.org/pre/abstract/10.1103/PhysRevE.49.3784>.
- [20] McSharry P. Nonlinear dynamics and chaos workshop. <http://people.maths.ox.ac.uk/mcsharry/lectures/ndc/ndcworkshop.shtml> (accessed 08.09.2014).